13th Australasian Fluid Mechanics Conference
Monash University, Melbourne, Australia
13-18 December 1998

TURBULENT TRANSPORT OF THE REYNOLDS STRESSES IN A ROD-ROUGHENED BOUNDARY LAYER

R. J. Smalley*, P. Å. Krogstad+ and R. A. Antonia*

*Department of Mechanical Engineering
University of Newcastle, N.S.W., 2308, Australia
+Department of Mechanics, Thermo and Fluid Dynamics
Norwegian University of Science & Technology, N-7034 Trondheim, Norway

ABSTRACT

Third-order velocity moments of velocity fluctuations were measured over a two-dimensional rod-roughened wall and compared with results obtained previously over different rough walls. Distinct differences below $y/\delta \sim 0.6$ were observed between the rod-roughness and other rough walls, even when the roughness function did not change. The loss of turbulent kinetic energy by diffusion exhibited in the wall region over most rough surfaces contrasts with the gain observed over the rod-roughness.

INTRODUCTION

Although there is considerable literature on turbulent boundary layers over rough walls, the roughness is described only in terms of the effect it has on the mean velocity profile. There are reasons to believe that this description is oversimplified and unrealistic.

Townsend's (1976) similarity hypothesis proposed that, outside the roughness sublayer ($\simeq 5$ times the roughness height) the flow is independent of wall roughness at sufficiently high R_θ. From profiles of the second-order velocity moments $\langle v^{+2} \rangle$ and $-\langle u^+ v^+ \rangle$, Krogstad et al. (1992) observed that effect of the roughness extends well into the outer region, by comparison to a smooth wall layer. This suggested there is important communication between the inner and outer layers above a rough wall, in contradistinction with the similarity hypothesis. In the present work, we focus on third-order velocity moments, primarily those which appear in the diffusion term of the transport equation for the Reynolds stresses. We compare measurements over various rough walls with nominally the same roughness function (ΔU^+). These include a wire mesh roughness (Krogstad et al., 1992), a sandpaper roughness (Andreopoulos & Bradshaw, 1981) and new results obtained over a 2-D rod-roughness.

In addition to turbulent boundary layers with similar ΔU^+, more general comparisons are made. One is between the 2-D roughness of Bandyopadhyay and Watson (1988) which has a similar ratio of the streamwise spacing to roughness element height, (p/k) as the rod-roughened wall. The other is between surfaces of completely different geometry. Reference to smooth walls is made using the data of Andreopoulos and Bradshaw (1981) and Spalart (1988).

EXPERIMENTAL DETAILS

The wind tunnel was described in Krogstad et al. (1992). The test surface consisted of a rough wall made from parallel rods spanning the width of the section and extending between 0.17 and 3.17 m from the entrance of the working section. The boundary layer was tripped by a 4 mm diameter rod, followed by a 17 cm strip of No. 40 grit sandpaper, both spanning the width of the section. The centreline spacing between the rods was 4 times the rod diameter of 1.60 mm.

All results presented in this paper for the rod-roughened boundary layer are from measurements performed at $x = 2.03$ m with two X-wire probes. 2.5 μm diameter wires were etched to a nominal length of 0.5 mm from Pt-10% Rh Wollaston wire. In-house CTA anemometers set to an overheat ratio of 1.5 were used, and the signals from the X-wires were filtered through fourth-order-Butterworth filters at a cut-off frequency of 4 kHz. Before digitising, the signals were amplified to use the greatest possible input range of a 12 bit Boston Technology A/D converter and subsequently sampled for 25 s at 8 kHz into a NEC 386 personal computer.

A freestream velocity of 7 ms^{-1} was used to produce the same ΔU^+ which occurs over other rough walls. Further details relating to the measurement of the flow appear in Table 1. The friction velocity, u_τ, was estimated from a least squares fit of the velocity-defect form of the combined log-law and wake function to the measured velocity profile, as presented by Krogstad et al.

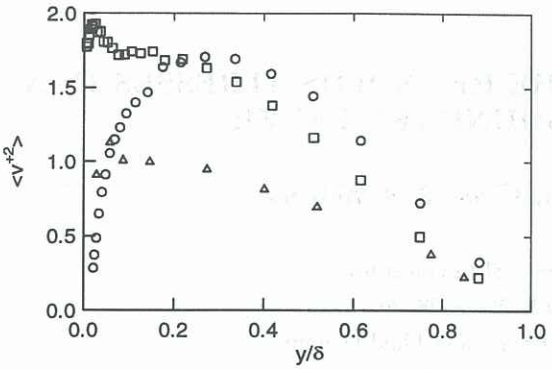

Figure 1: Normal Reynolds stress for rough walls with similar ΔU^+. ○, rod-roughness; □, wire mesh; △, sandpaper.

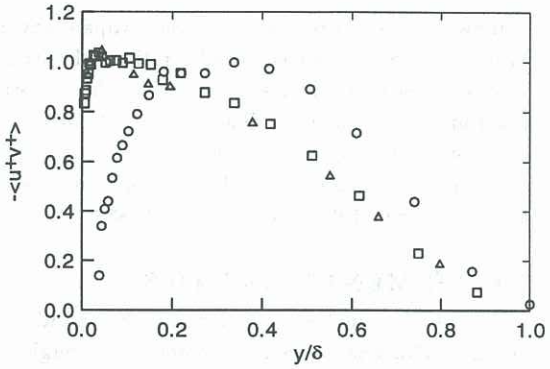

Figure 2: Reynolds shear stress for rough walls with similar ΔU^+. Symbols as in Figure 1.

THIRD-ORDER VELOCITY MOMENTS

The influence of the roughness on the turbulence can be first highlighted through a comparison of the $\langle v^{+2} \rangle$ and $-\langle u^+ v^+ \rangle$ profiles (Figures 1 and 2 respectively) between rough wall layers, in particular those with similar ΔU^+. For various rough walls, the flow and roughness characteristics are presented in Table 1. Significant differences are noted between the Reynolds stresses presented. There is no region of constant shear stress close to the wall for the rod roughness, and there is practically no similarity in the $\langle v^{+2} \rangle$ distributions between different rough surfaces. The measured non-zero third-order velocity moments for the rod-roughened turbulent boundary layer are presented in Figure 3. Further investigated are the moments with a significant contribution to the diffusion of turbulent kinetic energy (TKE) and Reynolds shear stress, viz. only the wall-normal gradients of the triple products are considered. $\langle u^{+2} v^+ \rangle$ and $\langle v^{+3} \rangle$ are presented in Figures 4 and 5 respectively, while $\langle w^{+2} v^+ \rangle$, although significant, is not measured with conventional X-wires and is approximated using $\frac{1}{2}[\langle u^{+2} v^+ \rangle + \langle v^{+3} \rangle]$.

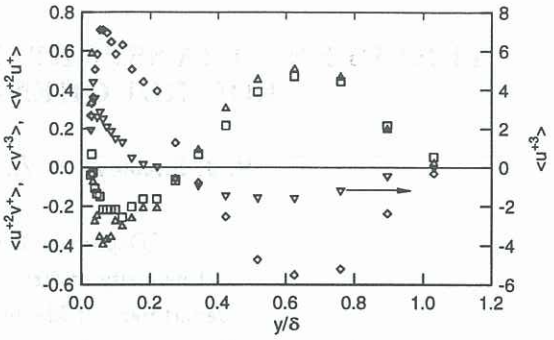

Figure 3: Third-order velocity moments for the rod-roughened wall. ▽, $\langle u^{+3} \rangle$; △, $\langle u^{+2} v^+ \rangle$; □, $\langle v^{+3} \rangle$; ◇, $\langle v^{+2} u^+ \rangle$.

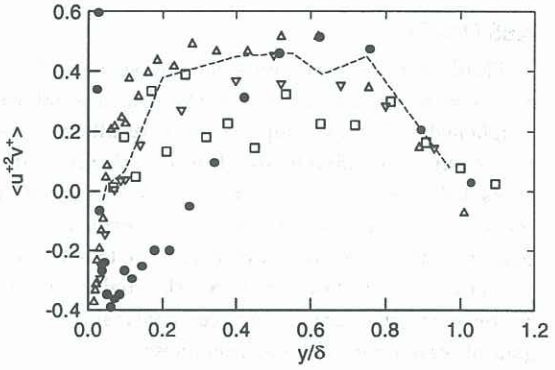

Figure 4: Third-order velocity moment $\langle u^{+2} v^+ \rangle$ for various wall surfaces. ●, rod-roughness; ▽, sandpaper; △, wire mesh; □, transverse bar; - -, smooth wall.

For the rod-roughness, $\langle u^{+2} v^+ \rangle$ and $\langle v^{+3} \rangle$ are both negative until y/δ exceeds 0.3. For the wire mesh, sandpaper and gravel rough walls, $\langle u^{+2} v^+ \rangle$ is negative only near the surface, while $\langle v^{+3} \rangle$ is entirely positive. For the 2-D transverse bar roughness $\langle u^{+2} v^+ \rangle$ and $\langle v^{+3} \rangle$ are positive throughout the layer.

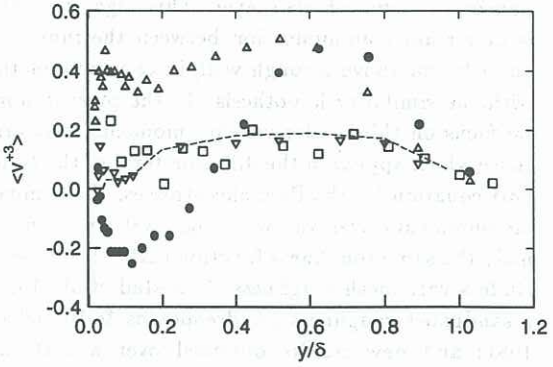

Figure 5: Third-order velocity moment $\langle v^{+3} \rangle$ for various wall surfaces. Symbols as in Figure 4.

Table 1. Flow Quantities and Roughness Characteristics of the Rough Walls Investigated

Wall Type	Author	R_θ	ΔU^+	p/k
Rods	Present	4810	11.4	4
Wire mesh	Krogstad et al. (1992)	12800	11.0	N/A
Sandpaper	Andreopoulos and Bradshaw (1981)	$O(10^4)$	10.5	N/A
2-D transverse square bar	Bandyopadhyay and Watson (1988)	2890	8	3.8
Gravel[a]	Mulhearn and Finnigan (1978)	—	—	N/A
Crop canopy[a]	Maitani (1979)	—	—	N/A

[a]Results not presented in this paper

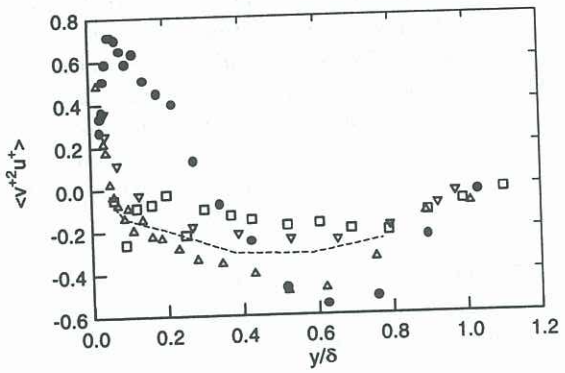

Figure 6: Third-order velocity moment $\langle v^{+2}u^+\rangle$ for various wall surfaces. Symbols as in Figure 4.

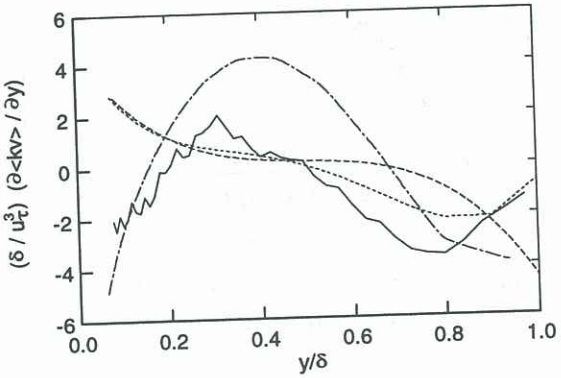

Figure 7: TKE diffusion for various wall surfaces. — - —, rod-roughness; – –, sandpaper; - - -, wire mesh; —, smooth wall.

Apart from the rods and the wire mesh roughness, differences in magnitude exist between the third-order velocity moments over the same rough wall. For the smooth wall and sandpaper roughness, $\langle u^{+2}v^+\rangle$ is twice $\langle v^{+3}\rangle$ for most of the layer, and over the 2-D transverse bar roughness $\langle u^{+2}v^+\rangle$ is slightly larger than $\langle v^{+3}\rangle$.

The moment $\langle v^{+2}u^+\rangle$, associated with the diffusion of the Reynolds shear stress, is presented in Figure 6. Over the rod-roughness, the distribution is positive for $y/\delta \lesssim 0.3$. The magnitudes of the near-wall peak and of the local minima between y/δ of 0.6 and 0.7 are also increased. For the sandpaper, wire mesh and gravel roughnesses, $\langle v^{+2}u^+\rangle$ decreases rapidly near the wall, although for the wire mesh roughness, there is an increase in magnitude in the outer layer. For a smooth wall, there is no region where $\langle v^{+2}u^+\rangle$ is positive. The distribution over the 2-D transverse bar roughness is also completely negative, although there is a near-wall minimum at $y/\delta \simeq 0.1$ which does not appear over other wall surfaces.

TKE DIFFUSION

The diffusion shown in Figure 7 for the rough walls was calculated from

$$\frac{3}{4}\,\frac{\partial(\langle u^2v\rangle + \langle v^3\rangle)}{\partial y}\ .$$

Results close to the wall ($y/\delta \lesssim 0.05$) were ignored as hot wire anemometry is not reliable in this region (LDV would be a better technique). The smooth wall diffusion is from the TKE budget ($R_\theta = 1410$) of Spalart (1988), and contains all terms associated with the TKE diffusion.

For the rod-roughness, there is considerably greater diffusion throughout the entire layer than for the other surfaces. This is due to the increased gradients which result from the large maxima and minima occurring in the distributions of $\langle u^{+2}v^+\rangle$ and $\langle v^{+3}\rangle$. There is a notable difference in diffusion within the inner region between the rod roughness and most of the other rough walls (including results not presented over crop canopies and the gravel roughness). A gain of TKE by diffusion occurs below $y/\delta \leq 0.15$ for the rod-roughness, whereas there is a loss of TKE by diffusion throughout the majority of the inner layer for the other surfaces. For $0.15 \leq y/\delta \leq 0.5$, all surfaces have a loss of TKE by diffusion although for the rod roughness the magnitude is considerably greater.

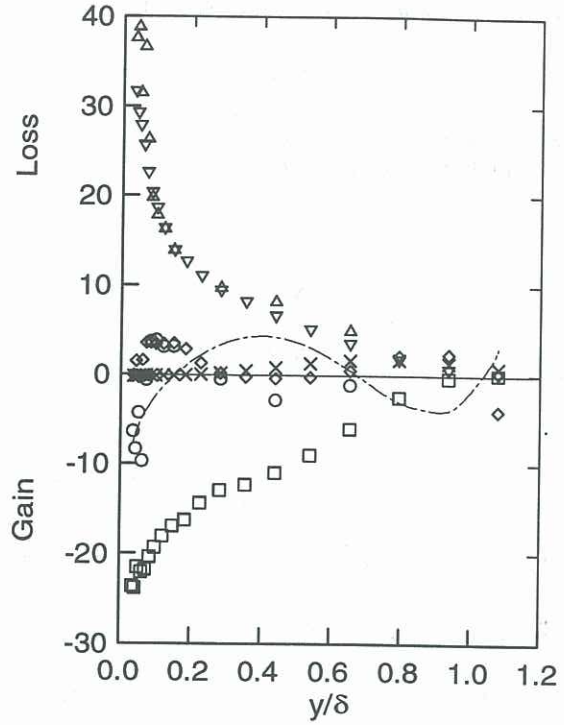

Figure 8: The TKE budget for the rod-roughened turbulent boundary layer. □, production; ▽, dissipation (isotropy); △, dissipation (u spectrum); — - —, diffusion; ×, advection; ◊, imbalance (isotropy); ○, imbalance (u spectrum).

The diffusion over the two-dimensional transverse bar was not determined due to the considerable scatter present in the third-order velocity moments. However, a diffusion distribution was presented by Antonia and Luxton (1971) over a similar rough wall ($p/k = 4$), where there was a gain of TKE by diffusion between y/δ of 0.1 and 0.5. This distribution is not similar to either the diffusion over the rod-roughness or the other rough walls.

Although the diffusion over the smooth wall of Spalart (1988) does not completely concur with the rod-roughness diffusion distribution, it appears to be a better comparison than over other walls, where a loss of TKE by diffusion occurs throughout the entire near-wall region.

TKE BUDGET

The transport equation for the TKE in a zero pressure gradient boundary layer can be approximated to

$$U\frac{\partial\langle k\rangle}{\partial x} + V\frac{\partial\langle k\rangle}{\partial y} = -\langle uv\rangle\frac{\partial U}{\partial y} - \frac{\partial\langle vk\rangle}{\partial y} - \epsilon \quad . \quad (1)$$

Figure 8 displays all the terms in (1) [non-dimensionalised by u_τ^3/δ] and also a resulting imbalance for the rod-roughened layer. The dissipation calculated by assuming isotropy is nearly equivalent to the value inferred from the u spectrum almost throughout the layer. Apart from the wall region, the level of imbalance is tolerable, indicating that the diffusion obtained from using the assumption of $3/2[\langle u^{+2}v^{+}\rangle + \langle v^{+3}\rangle]$ is reasonable. It also meets the requirement that it should integrate to zero across the layer.

CONCLUSION

The distributions of third-order velocity fluctuation moments of the TKE diffusion for the rod-roughness differ considerably from distributions over the wire mesh and sandpaper roughnesses, although each have nominally the same ΔU^+. The magnitudes of the third-order moments over the wire mesh and rod-roughnesses are considerably increased by comparison with those for the sandpaper roughness. The moments also differ between other rough walls and the rod-roughness, including the 2-D transverse bar, where both have a similar p/k ratio. There is a gain of turbulent kinetic energy by diffusion in the near-wall region of the rod-roughness, contrary to results obtained over all other rough walls.

ACKNOWLEDGEMENT

The support of the Australian Research Council is gratefully acknowledged.

REFERENCES

ANDREOPOULOS, J. and BRADSHAW, P. 1981. Measurements of turbulence structure in the boundary layer on a rough surface, *Boundary-Layer Meteorol.*, **20**, 201-213.

ANTONIA, R. A. and LUXTON, R. E. 1971. The response of a turbulent boundary layer to a step change in surface roughness. Part 1. Smooth to rough, *J. Fluid Mech.*, **48**, 721-761.

BANDYOPADHYAY, P. R. and WATSON, R. D. 1988. Structure of rough-wall turbulent boundary layers, *Phys. Fluids*, **31**, 1877-1883.

KROGSTAD, P. Å., ANTONIA, R. A. and BROWNE, L. W. B. 1992. Rough- and smooth-wall turbulent boundary layers, *J. Fluid Mech.*, **245**, 599-617.

MAITANI, T. 1979. A comparison of turbulence statistics in the surface layer over plant canopies with those over several other surfaces, *Boundary-Layer Meteorol.*, **17**, 213-222.

MULHEARN, P. J. and FINNIGAN, J. J. 1978. Turbulent flow over a very rough, random surface, *Boundary-Layer Meteorol.*, **15**, 109-132.

SPALART, P. R. 1988. Direct simulation of the turbulent boundary layer up to $R_\theta = 1410$, *J. Fluid Mech.*, **187**, 61-98.

TOWNSEND, A. A. 1976. *The Structure of Turbulent Shear Flow*, 2nd ed., Cambridge University Press.